

 **Very Important Publication**

Dual Photoredox and Nickel Catalysed Reductive Coupling of Alkynes and Aldehydes

Francesco Calogero,^{+a, c} Giandomenico Magagnano,^{+a, c} Simone Potenti,^{+b, c}
 Andrea Gualandi,^{a, c,*} Andrea Fermi,^{a, c,*} Paola Ceroni,^{a, c} and
 Pier Giorgio Cozzi^{a, c,*}

^a Dipartimento di Chimica “Giacomo Ciamician” Alma Mater Studiorum – Università di Bologna, Via Selmi 2, 40126 Bologna, Italy

Phone: 0039-0512099511

E-mail: andrea.gualandi10@unibo.it; andrea.fermi2@unibo.it; piergiorgio.cozzi@unibo.it

^b Laboratorio SMART, Scuola Normale Superiore, Piazza dei Cavalieri 7, 56126, Pisa, Italy

^c Center for Chemical Catalysis – C3, Alma Mater Studiorum – Università di Bologna, Via Selmi 2, 40126 Bologna, Italy

⁺ These authors contributed equally to this work.

Manuscript received: May 31, 2022; Revised manuscript received: June 28, 2022;

Version of record online: July 18, 2022



Supporting information for this article is available on the WWW under <https://doi.org/10.1002/adsc.202200589>

© 2022 The Authors. *Advanced Synthesis & Catalysis* published by Wiley-VCH GmbH. This is an open access article under the terms of the Creative Commons Attribution Non-Commercial NoDerivs License, which permits use and distribution in any medium, provided the original work is properly cited, the use is non-commercial and no modifications or adaptations are made.

Abstract: A regioselective vinylation of aromatic and aliphatic aldehydes promoted by the merging of photoredox and nickel catalysis is here reported. A comprehensive investigation on the reaction conditions allowed the disclosure of a valid and reproducible protocol based on a nickel-mediated reductive coupling approach under visible light irradiation. The employment of 3CzClIPN (2,4,6-tris(carbazol-9-yl)-5-chloroisophthalonitrile) as the photocatalyst and Hantzsch's ester as the sacrificial organic reductant replace the use of boron-, silicon- or zinc-based reducing agents, making this method a worthy alternative to the already known protocols. The developed mild reaction conditions allow the access to a wide range of substituents decorating both the aldehyde and the alkyne. Moreover, careful photophysical investigations shed light on the mechanism of the reaction.

Keywords: Metallaphotoredox catalysis; Nickel catalysis; Aldehydes; Vinylation; Regioselectivity

Introduction

The exploitation of electrophilicity of carbonyl compounds as a chemical handle for the formation of chemical bonds is a crucial methodology in the synthetic toolbox for both academic and industrial purposes.^[1] In this context, the introduction of differently decorated vinyl groups to aldehydes occupies a privileged position^[2] both because this chemical motif is present in many natural products, and because forthcoming functionalizations are possible.^[3]

While nearly three decades passed since its introduction, due to its unique chemo-selectivity

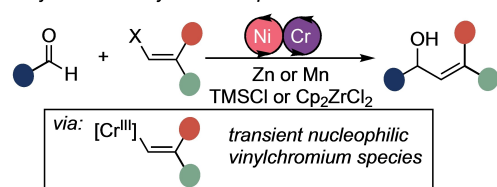
towards the aldehyde moiety, the catalytic variant of the Nozaki-Hiyama-Kishi reaction (NHK) still represents the benchmark methodology for the introduction of a vinyl group.^[4] However, although the NHK found ubiquitous applications over time, and both diastereo- and enantio-controlled variants still contribute to expand the tolerated functionalities on the molecular frameworks,^[5] a complementary approach is possible. The activation of easily available and abundant alkynes as masked alkene synthons can replace the use of (pseudo)halides. The vinylation product can be obtained, exploiting the extra π -linkage through a stepwise approach (hydrometallation followed by a

transmetalation step) in which two metal species act consecutively on terminal alkynes. In this scenario, various combinations of transition metals (e.g., [Zr]/[Al],^[6] [Zr]/[Zn],^[7] [B]/[Zn]^[8]) have proven to be effective also in stereocontrolled fashion (Figure 1).

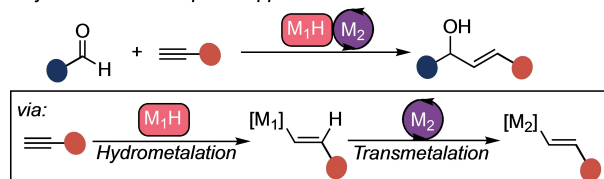
Alternatively, the C–C bond-forming step can occur with the concomitant formation of a metallacycle through a multicomponent reaction involving combination of alkyne, aldehyde, and a metal complex in low oxidation state. Although several metals in both stoichiometric and catalytic amounts have proven to promote this type of process (e.g., [Ti],^[9] [Ru]^[10] or [Rh]^[11]), the use of nickel played the central role in this area (Figure 2).^[12]

The catalytic version of these transformations concerns the formation of a new bond between the two π -coupling partners, in the presence of an appropriate nickel complex and a stoichiometric amount of a reducing agent (e.g., Et_2Zn ,^[13] R_3SiH ,^[14] BEt_3 ,^[15] BnOH ^[16]). In these reactions, normally, internal asymmetric alkynes are employed, and the formation of a nickel(II)cycle intermediate allows an almost complete control of the regioselective outcome of intermolecular process.^[17] Although this methodology was successfully extended to an enantio-selective variants even in the presence of other electrophiles (e.g., imines or epoxides)^[18,19] some non-negligible limitations remain. Since the nickel complex coordinating to both

Catalytic Nozaki-Hiyama-Kishi protocol



Alkyne activation: Stepwise approach



Alkyne activation: Oxidative cyclization

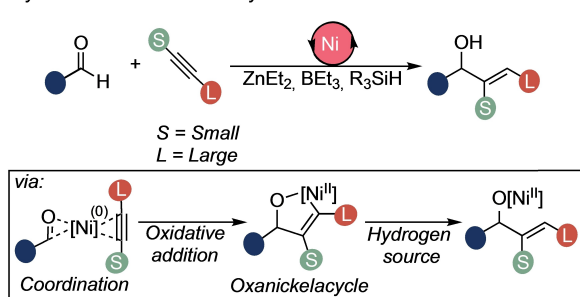
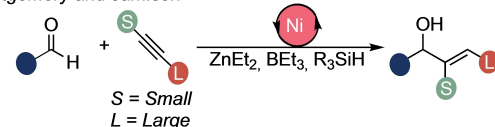


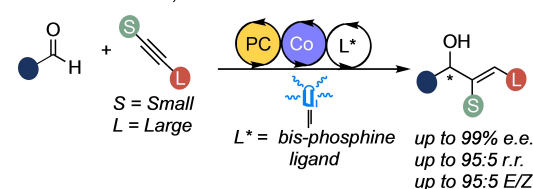
Figure 1. Classical transition metal catalysed vinylation.

Montgomery and Jamison



Photoredox methodologies

Xia and co-workers, 2021



This Work:

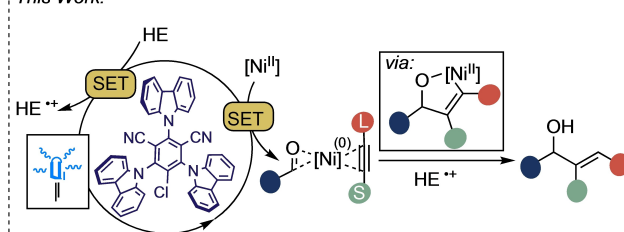


Figure 2. Transition metal catalysed vinylation.

carbonyl and alkyne must donate electronic density to ensure the oxidative cyclization, in most of the cases the catalytic system requires the use of the air sensitive $\text{Ni}(\text{COD})_2$. Moreover, the use of over-stoichiometric reductants is mandatory to reduce the nickel(II)cycle to $\text{Ni}(0)$, closing the catalytic cycle and forming the corresponding alkoxy derivative (OM, with $\text{M} = \text{ZnEt}$, BEt_2 , or SiEt_3). In some cases, functional groups are not compatible with the above-mentioned stoichiometric reducing agents. Finally, the regioselectivity of reductive cross coupling was unsatisfactory with disubstituted alkynes with groups of similar steric hindrance.

In the last decade dual metalla-photoredox catalysis, that is the combination of metal-promoted processes with photoredox cycles, has reached an extraordinary level of advancement.^[20] The synergistic use of two different molecule activation method allowed the resolution of several problems, affecting the most employed methods in organic synthesis. For instance, examples of diastereoselective and enantioselective allylation of aldehydes through a combination of photoredox and chromium(II) in a Reductive Radical Polar Cross-Over (RRPCO)^[21] approach were reported independently by Glorius and Kanai.^[22] Our laboratory is long-standing engaged in the development of methodologies for the functionalization of carbonyl compounds, towards the photoredox generation of transient nucleophilic organometallic species.^[23] Until now our research exploited net-reductive photoredox systems for the utilization of

transition metals in low oxidation state without the use of external metal reductants or scavengers in a more sustainable and less wasteful approach.

However, the access to a dual catalysed vinylation of aldehydes was so far prevented. In this sense, during the development of this project, Xia and co-workers reported a Co-catalysed reductive coupling of alkynes and aldehydes under visible light irradiation (Figure 2).^[24] The excellent regio- and enantio-selectivity of the process is achieved through the oxidative cyclization step allowed by the chiral cobalt complex. The use of a photoredox system (photocatalyst/organic reductant) allows the continuous reduction of the metal catalyst avoiding the presence of a (semi)metallic reductant. Although it represents a powerful proof-of-concept, the method is not applicable to alkynes other than 1-phenyl-1-propyne.

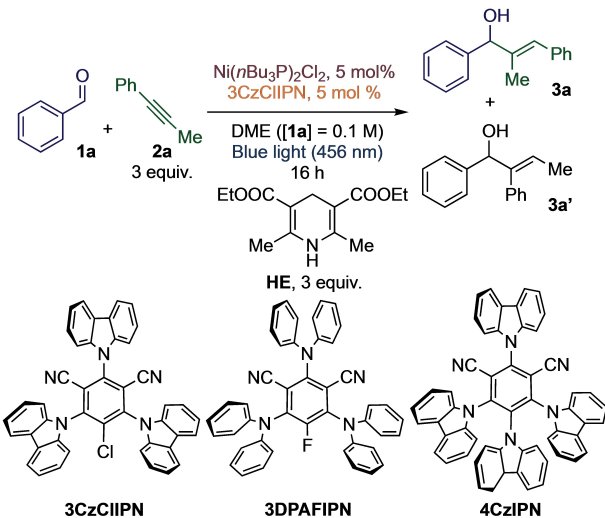
Another interesting approach towards the formation of reactive organometallic allyl-nickel reagents prepared under photoredox conditions was described by Xia^[25] who reported the Ni-catalysed reductive coupling of aldehydes with available 1,3-dienes. In the protocol Hantzsch's ester is used as the hydrogen radical source to oxidize low-valent nickel salt affording Ni–H species. Similarly, but using allenes, Breit^[26] developed an allylation methodology via a π -allylnickel intermediate obtained through insertion of allenes with a Ni–H intermediate.

Herein a dual photoredox and nickel catalysed vinylation of aromatic and aliphatic aldehydes is presented. Our protocol employs the easily synthesizable 3CzCIIPN (2,4,6-tris(carbazol-9-yl)-5-chloroisophthalonitrile)^[27] as the photocatalyst and Hantzsch's ester as the sacrificial reductant (Figure 2). Through the use of a preformed, bench-stable and commercially available nickel(II) catalyst, we have established a valid, reproducible, and regioselective photoredox vinylation protocol. The mild reaction conditions, the wide range of tolerated substituents decorating both the aldehyde and the alkyne, and the absence of boron, silicon or zinc based reducing agents make the method a worthy alternative to the already known protocols.

Results and Discussion

The salient results obtained during the optimization of the reaction conditions are summarized in the Table 1. Benzaldehyde (**1a**) and 1-phenyl-1-propyne (**2a**) were chosen as model substrates for the preliminary investigation. To enable the use of light radiation as a chemical energy source and to overcome the use of stoichiometric metal reductants or air sensitive nickel(0) sources, we focused our investigation on the class of thermally activated delayed fluorescence (TADF) organic dyes based on carbazolyl and diphenylamine substituted cyanoarenes,^[27,28] avoid the employ-

Table 1. Optimization studies.



Entry ^[a]	Deviations from standard conditions	Yield %	3a:3a' ^[b]
1	none	71	92:8
2	No [Ni]	–	–
3	No light	–	–
4	No PC	–	–
5	3DPAFIPN instead of 3CzCIIPN	28	93:7
6	4CzIPN instead of 3CzCIIPN	68	92:8
7	[NiCl ₂ (<i>n</i> Bu ₃ P) ₂] 2.5 mol%	36	92:8
8	[NiCl ₂ (<i>n</i> Bu ₃ P) ₂] 10 mol%	68	90:10
9	[NiCl ₂ (<i>n</i> Bu ₃ P) ₂] 15 mol%	30	82:18
10 ^[c]	[NiCl ₂ (<i>n</i> Bu ₃ P) ₂] 10 mol%	35	86:14
11	[NiCl ₂ (<i>n</i> Bu ₃ P) ₂] 10 mol% and THF instead of DME	36	79:21
12 ^[d]	THF instead of DME	64	82:18
13 ^[d]	DCM instead of DME	–	–
14 ^[d]	DMF instead of DME	–	–
15 ^[d]	MeCN instead of DME	–	–
16 ^[d]	DME [1a = 0.05 M]	40	89:11
17 ^[d]	TEA instead of HE	–	–
18	[NiCl ₂ (Et ₃ P) ₂] 10 mol% instead of [NiCl ₂ (<i>n</i> Bu ₃ P) ₂]	35	85:15
19	NiCl ₂ (glyme) 10 mol% and PCy ₃ 15 mol% instead of [NiCl ₂ (<i>n</i> Bu ₃ P) ₂]	–	–
20	NiCl ₂ (glyme) 10 mol% and dtbbpy 15 mol% instead of [NiCl ₂ (<i>n</i> Bu ₃ P) ₂]	–	–
21	NiCl ₂ (glyme) 10 mol% and <i>o</i> -phen 15 mol% instead of [NiCl ₂ (<i>n</i> Bu ₃ P) ₂]	–	–

^[a] Reaction performed on a 0.2 mmol scale. Isolated yield after chromatographic purification. TEA = Triethylamine; HE = Hantzsch ester.

^[b] Determined by ¹H-NMR analysis of the reaction crude. *E/Z* > 95:5.

^[c] 6 hours irradiation time.

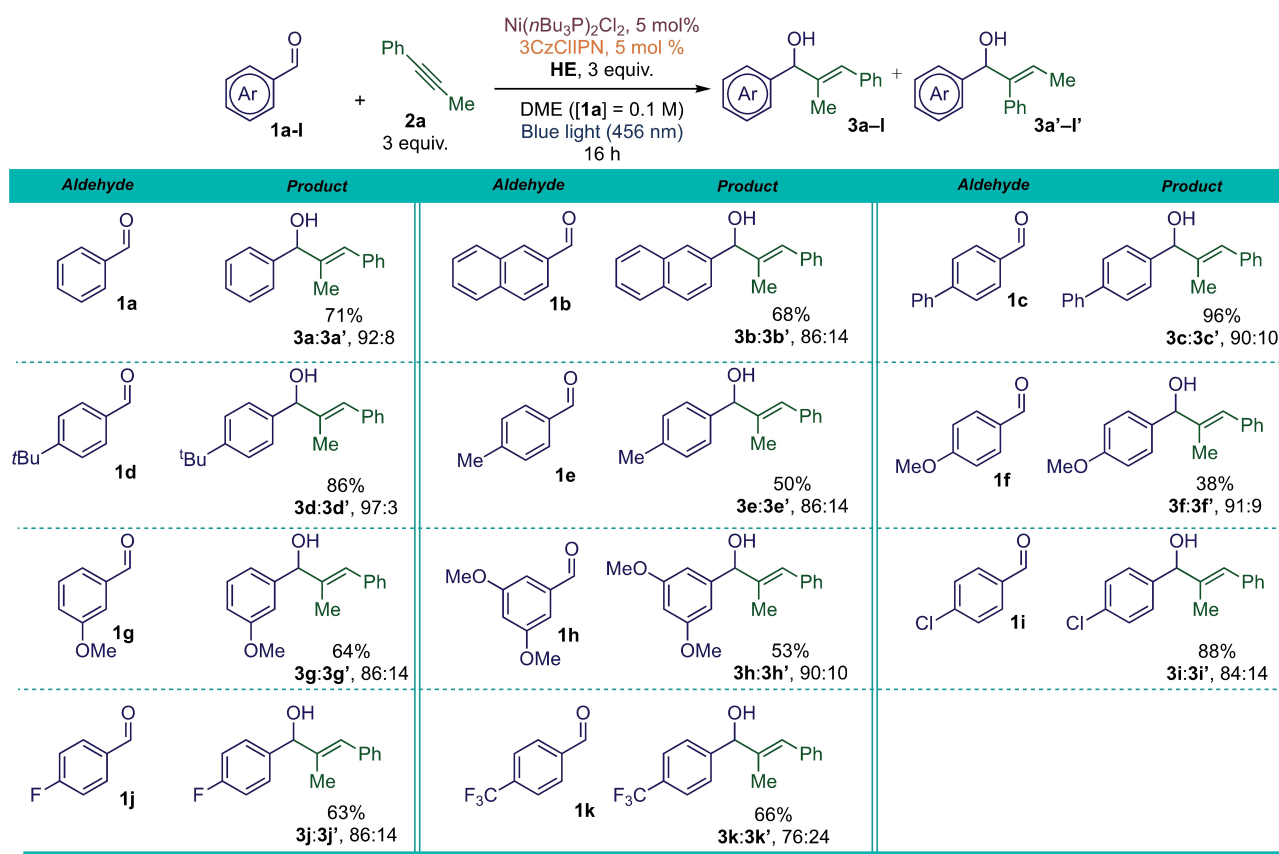
^[d] NiCl₂(*n*Bu₃P)₂ 10 mol%.

ment of metal photocatalysts based on iridium and ruthenium. Among all possible candidates, 3CzCIIPN was chosen in combination with the diethyl Hantzsch's ester (**HE**) that was employed as organic reductant. Although this dye is less used than other analogues, (e.g., 4CzIPN, or 3DPAFIPN) it exhibits important properties for its use in dual photoredox and nickel-promoted reductive processes. The values of the available reduction potential both for the ground and for the excited state of 3CzCIIPN are lower than the ones reported for the most commonly employed 4CzIPN, or 3DPAFIPN (excited state potentials of the mentioned photocatalysts vs SCE: $E(4CzIPN^*/4CzIPN) = -1.18$ V; $E(3DPAFIPN^{*+}/3DPAFIPN) = -1.38$ V; $E(3CzCIIPN^{*+}/3CzCIIPN) = -0.93$ V; reduction potential of ground state of the photocatalysts vs SCE: $E(4CzIPN/4CzIPN^*) = -1.24$ V; $E(3DPAFIPN/3DPAFIPN^*) = -1.59$ V, while $E(3CzCIIPN/3CzCIIPN^*) = -1.16$ V).

The mild reducing properties of 3CzCIIPN disfavours direct reductions of aromatic aldehydes, thus minimizing the parasitic pinacol coupling that may occur with aromatic aldehydes in the presence of strong reducing photocatalysts and oxidized Hantzsch's ester. For the selection of the most appropriate nickel catalyst, based on the important previous work done by Jamison and Montgomery,^[13–15,17,19] we selected stable and commercially available dichlorobis(tributylphosphine)nickel(II) $[NiCl_2(nBu_3P)_2]$, used in an initially catalytic loading of 10% mol (Table 1, entry 10). At the same time, to ensure the turnover of the photoredox catalytic cycle, three equivalents of **HE** were used in THF as solvent. After 6 hours of reaction, the desired product was isolated with 35% yield, a complete *E*-selectivity, and a moderate regio-selectivity of 79:21 in favour of the same regioisomer observed for non-light driven protocols. To our delight, a significant increase in yield was appreciated increasing the irradiation time from 6 to 16 hours and product **3a** was isolated in 64% yield (Table 1, entry 11). The regioselectivity of the reaction was improved by changing the reaction solvents (Table 1, entries 12–14). We observed that a better regioselectivity was obtained in coordinating solvents. In this sense, moving from THF to the slightly more polar DME (Table 1, entry 7), it was possible to isolate the desired product, improving both the yield and the regioselective outcome (68% yield, 90:10 for **3a**:**3a'**). Regarding the nickel complex (Table 1, entries 17–20), as was previously reported, the presence of strong σ -donating phosphine is mandatory to observe a positive outcome of the reaction. Commonly employed nitrogen ligands such as bipyridine, phenanthroline, bis-oxazolines, quite active in many photoredox processes mediated by nickel, failed to promote the reaction. Similarly, the same unsatisfactory results were obtained testing triaryl phosphine ligands. When $[NiCl_2(Et_3P)_2]$ was employed, inferior

results were obtained. In this case, carrying out the reaction the isolated yield was modest (35%), with a regioselectivity that was 85:15. Once it was verified that the initially employed $[NiCl_2(nBu_3P)_2]$ was the best catalyst, its loading was further optimized. By increase of the catalysts loading to 15 mol%, we have observed both a diminished yield and lower regioselectivity (Table 1, entry 8). This could be related to the absorption properties of the $[NiCl_2(nBu_3P)_2]$, that possess an absorption band in the blue region of the spectrum ($\epsilon_{455nm} \approx 370$ M⁻¹ cm⁻¹, see SI for complete photophysical details) and a significant amount of the blue photons were absorbed, preventing excitation of the photocatalyst. The presence of photocatalyst is, on the other hand, indispensable to the reaction, as the $[NiCl_2(nBu_3P)_2]$ alone under blue light irradiation gave no reaction. Further supporting this photophysical evidence, it was possible to improve the results obtained by decreasing the catalytic loading of $[NiCl_2(nBu_3P)_2]$ to 5% mol (Table 1, entry 1), resulting in a cleaner reaction crude, and improving the regioisomeric ratio. Three equivalents of alkyne and Hantzsch's ester are necessary for a smooth outcome of the reaction. The amount of alkyne could not be decreased for concomitant cyclotrimerization, promoted by nickel in low oxidation state.

After the systematic evaluation of all reaction parameters, we obtained **3a** in 71% isolated yield after 16 hours of irradiation, as single *E* isomer. Using the selected reaction conditions, we have investigated the possibility to employ differently decorated aromatic aldehydes with **2a** (Scheme 1). In general, quite different functional groups are compatible with our protocol. The presence of phenyl (**1c**) and the *tert*-butyl group (**1d**) allowed to obtain the corresponding allylic alcohol with high yields and a regioselective ratio higher than 90:10, demonstrating that the presence of bulky substituents in *para* position of the aromatic ring has a beneficial effect in the regioselectivity of the reaction. In contrast, aldehydes characterized by the presence of electron-donating substituents (**1f–h**) were found less reactive and a significant drop in yield was observed. Probably, the different reactivity can be imputable to the more electron rich character of the carbonyl group, that affects the kinetics of nickelacycle formation. However, positive results in terms of regioselective ratio were still recorded.^[29] For instance, when *p*-methoxy benzaldehyde (**1f**) was tested in the reaction, the vinylated product was isolated in 38% yield and with a regioselectivity of 91:9. Although, analysis of the crude reaction mixture revealed the presence of unreacted aldehyde, extending the irradiation time did not lead to a yield improvement caused the concurrent cyclotrimerization of the alkyne. Electron-poor aldehydes (**1i–k**), on the other hand, were found to be particularly more reactive, with a slight decrease in the regioisomeric control. The same



Scheme 1. Regioselective vinylation of aromatic aldehydes promoted by visible light and nickel catalysis.

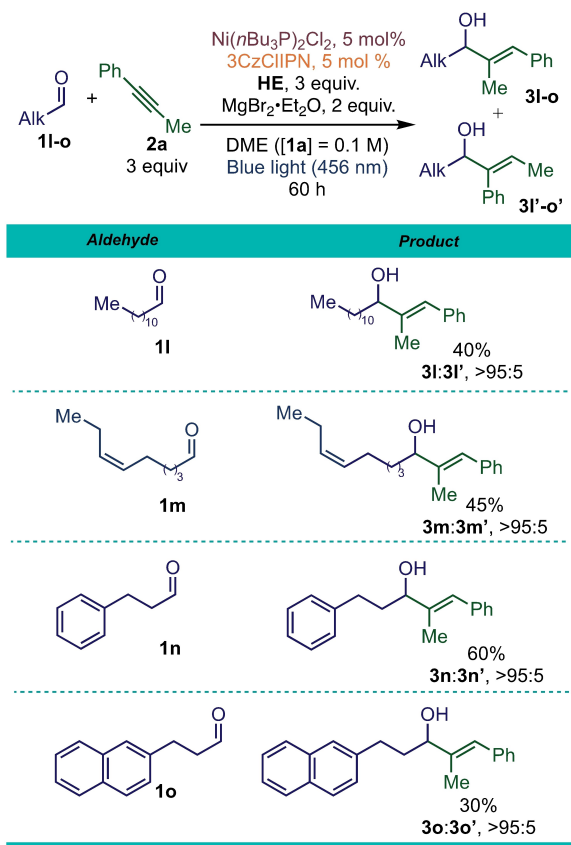
behavior was also observed when aliphatic aldehydes were examined, even though with a limited reactivity. Applying the best reaction conditions in the presence of aliphatic aldehydes **11–o**, it was only possible to observe the formation of the vinylated product with poor yields. Strong Lewis acids are reported to accelerate the oxidative cyclization step with both alkynes and alkenes by coordination of the aldehyde in the transition state.^[30]

To extend the applicability and the generality of the protocol, the presence of a Lewis acid capable of activating the carbonyl center^[31] and compatible with the photoredox conditions was crucial. Among the various Lewis acids and additives examined (see SI for details), the use of two equivalents of $\text{MgBr}_2 \cdot \text{Et}_2\text{O}$ allowed the access to vinylation of aliphatic substrates. The presence of $\text{MgBr}_2 \cdot \text{Et}_2\text{O}$ besides activating the carbonyl center for the oxidative cyclization step, has also an effect on the formation of the alkyne cyclization product. The presence of this additive limits the trimerization of alkyne, allowing also to extend the irradiation time. We have further investigated if the presence of $\text{MgBr}_2 \cdot \text{Et}_2\text{O}$ is beneficial for the reaction where poor results were obtained with aromatic aldehydes. Unfortunately, the reaction of **1f** with **2a**, in the new reaction conditions, gave the

pinacol of aldehyde as the only product. The difference in the behavior between aliphatic and aromatic aldehydes can be found in the lower reduction potentials of the latter in the presence of $\text{MgBr}_2 \cdot \text{Et}_2\text{O}$ that allow the formation of the corresponding ketyl radicals by the photocatalyst. With the reaction conditions in our hand, we decided to briefly investigate the dual Ni/photoredox vinylation protocol in the presence of selected aliphatic aldehydes (Scheme 2). To our delight, vinylation products were obtained with satisfactory yields by extending the reaction time to 60 hours. In all cases a single regioisomer was detected in the reaction crude.

While analyzing the survey of suitable substrates, we also faced some limitations. Heteroaromatic aldehydes such as 2-thiophene carboxaldehyde or 2-pyridine carboxaldehyde are not reactive substrates, probably due to nickel coordination. In addition, unsuccessful results were observed in the presence of substrates with a limited stability in acidic conditions (in our case, deriving from the pyridinium ion generated after oxidation of **HE**).^[23a]

Likewise, when we turned our attention to compatible alkynes, we found that it was not possible to extend the method to either terminal (*e.g.*, 1-hexyne) or internal alkynes carrying two aromatic or two



Scheme 2. Regioselective vinylation of aliphatic aldehydes promoted by visible light and nickel catalysis.

aliphatic moieties (e.g., 4-octyne or diphenylacetylene were found unreactive). In these cases, we do not have observed the desired product. In the presence of dialkylsubstituted acetylenes we have observed the trimerization of alkynes (mixtures of isomers). The fast trimerization of alkyne promoted by Ni(0) is overriding the coordination of aldehydes, probably due to the better donor ability of alkyne. With diphenylacetylene in addition to the trimerized product, we have also observed the reduction of the aromatic aldehyde to the corresponding alcohols. By contrast, successful results were obtained considering differently 2-substituted 1-phenylacetylenes. For the survey of these substrates, we selected 4-chloro benzaldehyde (**1i**) under the conditions applied for aromatic aldehydes (Scheme 3). To our delight, we found that several alkyl-phenylacetylenes are compatible with our conditions and good regioisomeric ratios, always in favor of the α -alkyl substituted allylic alcohols, were observed. The observed yields are slightly lower than the ones observed with **2a** but different substituents on the aryl portions are tolerated. Also in this case, the employment of a quite large excess of alkyne proved to be essential. Noteworthy, in analogy with recently reported data for similar reaction conditions,^[32] the

byproduct mainly detected, by GC-MS of the reaction crude, was an *E/Z* mixture of the alkene derived by reduction of the alkyne. Although long-chained alkyl-phenylacetylenes have been only marginally considered in the previous reports of nickel mediated reductive coupling of alkynes and aldehydes,^[31] we found these substrates suitable in our conditions. In this regard, Jamison, and co-workers, reported few examples of the employment of these substrates in the nickel catalysed reductive coupling. An intramolecular version of the reaction was used in a late stage macrocyclization for the total synthesis of Amphidinohde T1 and T4.^[31] It is worth mentioning that the dual photoredox cobalt catalysed protocol reported by Xia and co-workers could be not extended to these substrates.^[24]

Photophysical Investigation and Mechanistic Proposal

A thorough investigation on the photophysical properties of the organic dye has been conducted to gain insights into the reaction mechanism. In air-equilibrated DME at room temperature, the lower energy-lying electronic transition of 3CzClIPN is detected in the visible spectrum, giving rise to a broad and unstructured absorption band between ca. 335 and 480 nm ($\epsilon_{370\text{nm}} = 16900 \text{ M}^{-1} \text{ cm}^{-1}$), while its luminescence is peaked at 543 nm (Figure 3A; corresponding $E_{0-0} = 2.67 \text{ eV}$, see Figure S3, SI), in agreement with what observed for other carbazolyl derivatives of

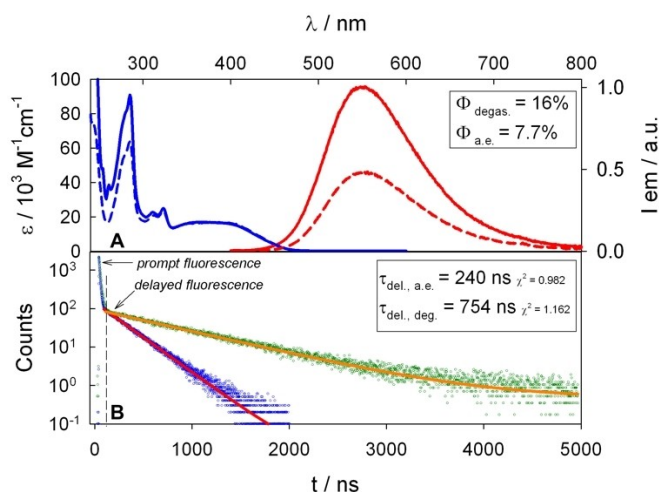
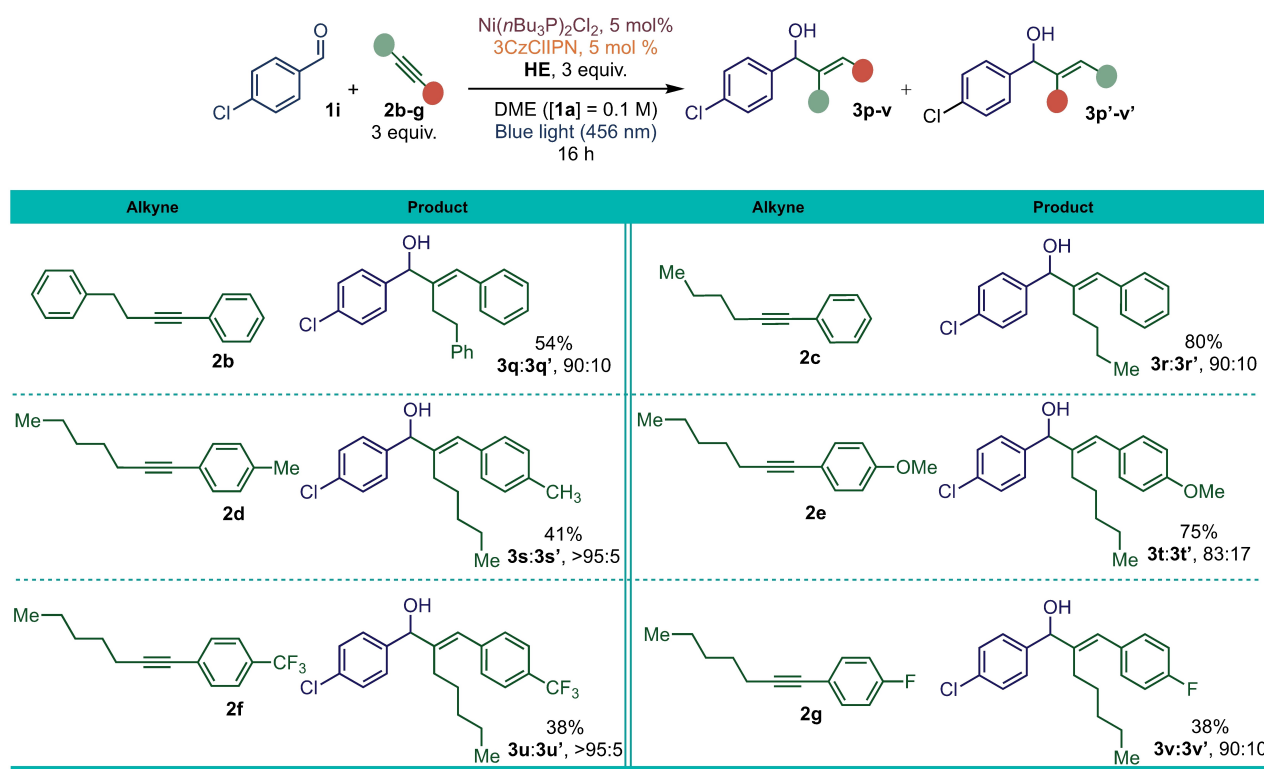


Figure 3. A: absorption (blue line) and comparison between emission spectra (red lines, corrected) of 3CzClIPN in oxygen-free (red line) and air-equilibrated (red dashed line) DME at r.t. ($\lambda_{\text{ex}} = 360 \text{ nm}$). The excitation spectrum is also shown as the blue dashed line ($\lambda_{\text{em}} = 570 \text{ nm}$). B: emission decays recorded in oxygen-free (green dots) and air-equilibrated (blue dots) solutions of 3CzClIPN in DME at r.t. The corresponding monoexponential fitting of the delayed fluorescence are shown as the red and orange lines, respectively.



Scheme 3. Regioselective vinylation promoted by visible light and nickel catalysis in presence of more decorated alkynes.

isophthalonitriles.^[27,32] Most interestingly, the emission quantum yield and decays are heavily affected by the presence of molecular oxygen. In oxygen-free solutions the quantum yield is 16%, compared to 7.7% in air-equilibrated solution, due to the increase of the reverse intersystem crossing efficiency (Φ_{RISC}). The emission intensities show a bi-exponential decays both in air-equilibrated and deoxygenated solutions at r.t. (Figure 3A).^[28a,33] Prompt and delayed fluorescence lifetimes are 13.1 and 754 ns, respectively in oxygen-free solution, while in air-equilibrated conditions both lifetimes are reduced to 9.5 and 240 ns, respectively (see Figure S4). No significant difference between the emission profiles obtained from air-equilibrated and oxygen-free solutions have been detected at r.t. In addition, in rigid matrix at 77 K ($\text{CH}_2\text{Cl}_2:\text{CH}_3\text{OH}$, 1:1 v/v) the emission profiles recorded with (50 μs) and without delay from the excitation pulse share the same maxima ($\lambda_{\text{max}} = 482$ nm, see Figure S5), suggesting that a significant decrease in temperature is negligibly affecting the relative energies of the lowest lying singlet (S_1) and triplet (T_1) excited states. Taken together, these observations most likely indicate a proximity in energy between the emitting singlet state S_1 and T_1 at r.t. (ΔE_{ST}), as recently highlighted in 3CzCIIPN neat films ($\Delta E_{\text{ST}} = 33$ meV).^[34] Considered all these important aspects, a careful analysis of the luminescence quenching of 3CzCIIPN in the presence

of the relevant reactants has been completed to obtain further information about a realistic mechanism of the light-driven reaction. Given its reduction potentials at the excited state ($E_{\text{red}}^{*/-} = 1.56$ V and $E_{\text{ox}}^{+/*} = \cong 0.93$ V vs. SCE in CH_3CN),^[27] 3CzCIIPN can perform thermodynamically favorable photo-induced electron transfer to oxidize **HE** ($E_0^{+/0} = 1.0$ V vs. SCE).^[35] In degassed solutions, additions of increasing amounts of **HE** lead to the highest quenching constant ($k_q = 5.9 \times 10^9 \text{ M}^{-1} \text{ cm}^{-1}$, see Figure S6–7), with the prompt fluorescence being negligibly quenched (see Figure S8).

Addition of nickel(II) complex $[\text{NiCl}_2(\text{nBu}_3\text{P})_2]$ in degassed CH_3CN ^[36] also results in the quenching of the delayed fluorescence of 3CzCIIPN (see Figure S9), with $k_q = 3.5 \times 10^9 \text{ M}^{-1} \text{ cm}^{-1}$. As expected, a similar quenching constant has been observed in air-equilibrated solutions, indicating that the presence of oxygen in this solvent does not chemically affect the complex (see Figure S10). On the other hand, no significant quenching phenomena have been observed on emission intensities of 3CzCIIPN upon additions of aldehyde **1a** or alkyne **2a** in degassed solutions (see Figure S12–13), most probably in reason of their high redox potentials (for **1a**: $E_0^{0/-} = -1.93$ V vs. SCE;^[37] for **2a**: $E_0^{+/0} > 2.0$ V vs. SCE).^[37]

By considering the concentrations of the reactants employed in the reaction, a comparison between

contributions of all substrates to the quenching efficiencies indicates that **HE** is the most probable quencher of the excited state of 3CzClIPN, with a quenching efficiency of ca. 99% (see Table S2). The formation of radical anion 3CzClIPN^{•-} ($E_0^{0/-} = -1.16$ V vs SCE in CH₃CN,^[27] via SET1, see Figure 4) allows the subsequent reduction of Ni(II) to Ni(I)^[38] (SET in Figure 4) and, most likely, of Ni(I) species to Ni(0) (SET II), which restores the chromophores in its starting neutral charge.

Based on the spectroscopical studies, and thanks to the insightful and careful analysis published on the reductive coupling of alkynes mediated by nickel in the presence of stoichiometric amount of reductant, we can propose a tentative catalytic cycle for the reaction (Figure 4). In previous reports, different mechanisms have been proposed for metal catalysed reductive coupling reactions.^[39] Jamison and Houk,^[30] and Montgomery and Houk^[40] have undertaken a mechanistic investigations of the process promoted by reductant such as BEt₃ or HSiR₃. The resting state of the catalyst was calculated being the 16e⁻ alkyne(bisphosphane) nickel(0) complex. Accordingly, we also propose the formation of the nickel(0) active catalyst in our photocatalytic reaction, by consecutive SET reactions (Figure 4). By the coordination of aldehyde and alkyne, the Ni(0) complex undergoes an oxidative cyclization forming the metallacycle. This step does not diverge from the reactions described by Jamison and Montgomery.^[30,40] The photoredox cycle is allowing the recycle of the nickel complex without using stoichiometric amount of Et₃B, ZnR₂, or HSiR₃. The interaction of HE^{•+} with the metallacycle is reducing the nickel complex,^[23d] that upon protonation, is

liberating the observed product and restore the nickel complex, that is successively reduced to the active Ni(0) specie.

Conclusion

We have disclosed a nickel mediated photoredox addition of alkyne to aldehydes without using organometallic reagents or hydrides in stoichiometric amounts. The methodology uses a stable and commercially available nickel complex, and the use of glove box to handle [Ni(COD)₂] is avoided. The reaction is regioselective and the employment of different alkyl substituted phenylacetylene derivatives is made possible. Aliphatic aldehydes display a reduced reactivity, and the reaction can be promoted by employing MgBr₂ as Lewis acid although with moderate yields. Further work toward an enantioselective photoredox variant is under active investigation in our laboratory.

Experimental Section

General Procedure: Dual Photoredox and Nickel Catalysed Reductive Coupling of Alkynes and Aromatic Aldehydes

All the reactions were performed on 0.2 mmol scale of aldehyde. A dry 10 mL Schlenk tube, equipped with a Rotaflo[®] stopcock, magnetic stirring bar and an argon supply tube, was charged under argon with Ni(*n*Bu₃P)₂Cl₂ (10 mol%, 0.01 mmol, 5.4 mg). Then, the substrate **1** (0.2 mmol), the organic photocatalyst 3CzClIPN (5 mol%, 0.01 mmol, 6.6 mg), diethyl 1,4-dihydro-2,6-diethyl-3,5-pyridinedicarboxylate Hantzsch's ester (3 equivalents, 0.6 mmol, 152 mg) were added. Freshly distilled inhibitor-free DME (2 mL in order to obtain a [I]=0.1 M

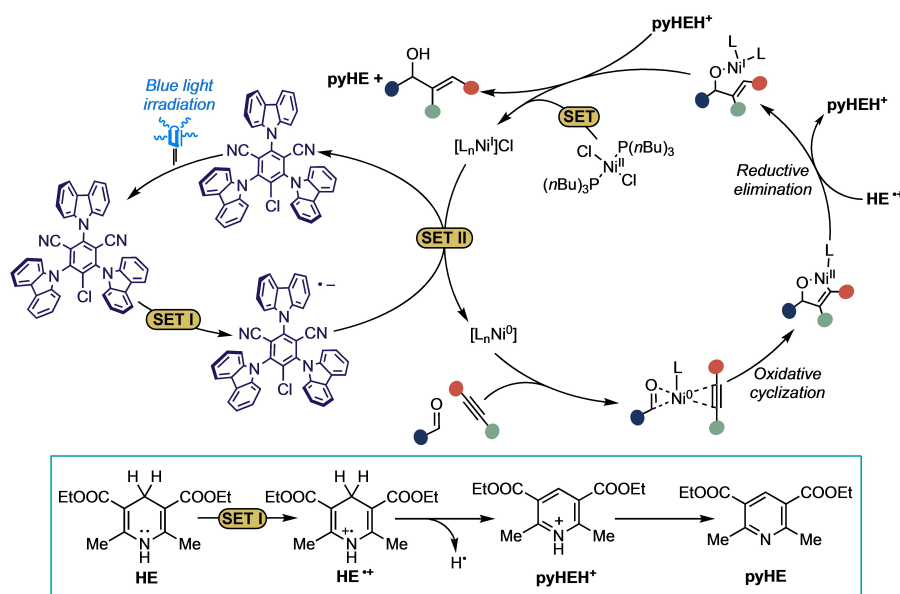


Figure 4. Proposed mechanistic picture for the photoredox nickel alkenylation of aldehydes.

substrate solution) was then added. The orange reaction mixture was allowed to stir for 5 min. and the alkyne **2a–g** was added dropwise to the solution. The reaction mixture was further subjected to a freeze-pump-thaw procedure (three cycles, two minutes each) and the vessel was refilled with argon. The reaction mixture was irradiated under vigorous stirring for 14 h and was quenched with water (approx. 4 mL) and extracted with AcOEt (4 × 3 mL). The combined organic layers were dried over anhydrous Na₂SO₄ and the solvent was removed under reduced pressure. The ¹H NMR of the reaction crude to evaluate the regioisomeric ratio, was recorded previous filtration over a small plug of celite with DCM. The crude was purified by flash column chromatography (SiO₂) to afford products **3** in the stated yields.

General Procedure: Dual Photoredox and Nickel Catalysed Reductive Coupling of Alkynes and Aliphatic Aldehydes

All the reactions were performed on 0.2 mmol scale of aldehyde. A dry 10 mL Schlenk tube, equipped with a Rotaflo[®] stopcock, magnetic stirring bar and an argon supply tube, was charged under argon with Ni(*n*Bu₃P)₂Cl₂ (10 mol%, 0.01 mmol, 5.4 mg). Then, the substrate **1** (0.2 mmol), the organic photocatalyst 3CzClIPN (5 mol%, 0.01 mmol, 6.6 mg), diethyl 1,4-dihydro-2,6-diethyl-3,5-pyridinedicarboxylate Hantzsch's ester (3 equivalents, 0.6 mmol, 152 mg) and MgBr₂•Et₂O (2 equivalents, 0.4 mmol, 103 mg) were added. Freshly distilled inhibitor-free DME (2 mL in order to obtain a [1]=0.1 M substrate solution) was then added. The orange reaction mixture was allowed to stir for 5 min. and the alkyne **2a–g** was added dropwise to the solution. The reaction mixture was further subjected to a freeze-pump-thaw procedure (three cycles, two minutes each) and the vessel was refilled with argon. The reaction mixture was irradiated under vigorous stirring for 14 h and was quenched with water (approx. 4 mL) and extracted with AcOEt (4 × 3 mL). The combined organic layers were dried over anhydrous Na₂SO₄ and the solvent was removed under reduced pressure. The ¹H NMR of the reaction crude to evaluate the regioisomeric ratio, was recorded previous filtration over a small plug of celite with DCM. The crude was purified by flash column chromatography (SiO₂) to afford products **3** in the stated yields.

Acknowledgements

P. G. C. acknowledges National project (PRIN 2017 ID: 20174SYJAF) SURSUMCAT "Raising up Catalysis for Innovative Developments" and the European Union's Horizon 2020 research and innovation programme under grant agreement No. 951996 for financial supports of this research. Open Access Funding provided by Università degli Studi di Bologna within the CRUI-CARE.

References

- [1] M. Schlosser, in *Organometallics in Synthesis: Third Manual*, Wiley: Hoboken, **2013**.
- [2] a) J. Montgomery, G. J. Sormunen, in *Metal Catalyzed Reductive C–C Bond Formation* (Ed.: M. J. Krische), Springer Berlin Heidelberg, Berlin, Heidelberg, **2007**, pp. 1–23; b) A. Lumbroso, M. L. Cooke, B. Breit, *Angew. Chem. Int. Ed.* **2013**, *52*, 1890–1932; *Angew. Chem.* **2013**, *125*, 1942–1986.
- [3] *Comprehensive Organic Synthesis. 1: Additions to C–X Pi-Bonds, Part I* (Ed.: Stuart L. Schreiber), Pergamon Pr., Oxford, **1993**.
- [4] A. Fürstner, N. Shi, *J. Am. Chem. Soc.* **1996**, *118*, 12349–12357.
- [5] a) Q. Tian, G. Zhang, *Synthesis* **2016**, *48*, 4038–4049; b) G. C. Hargaden, P. J. Guiry, *Adv. Synth. Catal.* **2007**, *349*, 2407–2424; c) Y. Gao, D. E. Hill, W. Hao, B. J. McNicholas, J. C. Vantourout, R. G. Hadt, S. E. Reisman, D. G. Blackmond, P. S. Baran, *J. Am. Chem. Soc.* **2021**, *143*, 9478–9488.
- [6] N. Okukado, E. Negishi, *Tetrahedron Lett.* **1978**, *19*, 2357–2360.
- [7] P. Wipf, W. Xu, *Tetrahedron Lett.* **1994**, *35*, 5197–5200.
- [8] W. Oppolzer, R. N. Radinov, *J. Am. Chem. Soc.* **1993**, *115*, 1593–1594.
- [9] a) A. B. Bahadoor, A. Flyer, G. C. Micalizio, *J. Am. Chem. Soc.* **2005**, *127*, 3694–3695; b) H. L. Shimp, G. C. Micalizio, *Org. Lett.* **2005**, *7*, 5111–5114.
- [10] R. L. Patman, M. R. Chaulagain, V. M. Williams, M. J. Krische, *J. Am. Chem. Soc.* **2009**, *131*, 2066–2067.
- [11] V. Komanduri, M. J. Krische, *J. Am. Chem. Soc.* **2006**, *128*, 16448–16449.
- [12] a) J. Montgomery, *Angew. Chem. Int. Ed.* **2004**, *43*, 3890–3908; *Angew. Chem.* **2004**, *116*, 3980–3998; b) S. Z. Tasker, E. A. Standley, T. F. Jamison, *Nature* **2014**, *509*, 299–309; c) E. Ortiz, J. Shezaf, Y.-H. Chang, M. J. Krische, *ACS Catal.* **2022**, *12*, 8164–8174.
- [13] J. Montgomery, *Acc. Chem. Res.* **2000**, *33*, 467–473.
- [14] a) S.-S. Ng, T. F. Jamison, *J. Am. Chem. Soc.* **2005**, *127*, 7320–7321; b) H. Wang, S. Negretti, A. R. Knauff, J. Montgomery, *Org. Lett.* **2015**, *17*, 1493–1496; c) A. J. Nett, S. Cañellas, Y. Higuchi, M. T. Robo, J. M. Kochkodan, M. T. Haynes, II, J. W. Kampf, J. Montgomery, *ACS Catal.* **2018**, *8*, 6606–6611; d) E. P. Jackson, J. Montgomery, *J. Am. Chem. Soc.* **2015**, *137*, 958–963.
- [15] a) K. M. Miller, W.-S. Huang, T. F. Jamison, *J. Am. Chem. Soc.* **2003**, *125*, 3442–3443; b) K. M. Miller, T. F. Jamison, *J. Am. Chem. Soc.* **2004**, *126*, 15342–15343; c) K. M. Miller, T. Luanphaisarnnont, C. Molinaro, T. F. Jamison, *J. Am. Chem. Soc.* **2004**, *126*, 4130–4131; d) A. D. Jenkins, A. Herath, M. Song, J. Montgomery, *J. Am. Chem. Soc.* **2011**, *133*, 14460–14466.
- [16] Y. Zheng, M. Ye, *Chin. J. Chem.* **2020**, *38*, 489–493.
- [17] P. R. McCarren, P. Liu, P. H.-Y. Cheong, T. F. Jamison, K. N. Houk, *J. Am. Chem. Soc.* **2009**, *131*, 6654–6655.

- [18] a) C.-Y. Zhou, S.-F. Zhu, L.-X. Wang, Q.-L. Zhou, *J. Am. Chem. Soc.* **2010**, *132*, 10955–10957; b) L. Li, Y.-C. Liu, H. Shi, *J. Am. Chem. Soc.* **2021**, *143*, 4154–4161.
- [19] C. Molinaro, T. F. Jamison, *J. Am. Chem. Soc.* **2003**, *125*, 8076–8077.
- [20] A. Y. Chan, I. B. Perry, N. B. Bissonnette, B. F. Buksh, G. A. Edwards, L. I. Frye, O. L. Garry, M. N. Lavagnino, B. X. Li, Y. Liang, E. Mao, A. Millet, J. V. Oakley, N. L. Reed, H. A. Sakai, C. P. Seath, D. W. C. MacMillan, *Chem. Rev.* **2022**, *122*, 1485–1542.
- [21] L. Pitzer, J. L. Schwarz, F. Glorius, *Chem. Sci.* **2019**, *10*, 8285–8291.
- [22] a) J. L. Schwarz, F. Schafers, A. Tlahuext-Aca, L. Lückemeier, F. Glorius, *J. Am. Chem. Soc.* **2018**, *140*, 12705–12709; b) J. L. Schwarz, H.-M. Huang, T. O. Paulisch, F. Glorius, *ACS Catal.* **2020**, *10*, 1621–1627; c) J. L. Schwarz, R. Kleinmans, T. O. Paulisch, F. Glorius, *J. Am. Chem. Soc.* **2020**, *142*, 2168–2174; d) F. Schafers, L. Quach, J. L. Schwarz, M. Saladrigas, C. G. Daniliuc, F. Glorius, *ACS Catal.* **2020**, *10*, 11841–11847; e) H.-M. Huang, P. Bellotti, C. Daniliuc, F. Glorius, *Angew. Chem. Int. Ed.* **2021**, *60*, 2464–2471; *Angew. Chem.* **2021**, *133*, 2494–2501; f) F. Schäfers, S. Dutta, R. Kleinmans, C. Mück-Lichtenfeld, F. Glorius, **2021**, <https://doi.org/10.26434/chemrxiv-2021-dvnlb>; g) H. Mitsunuma, S. Tanabe, H. Fuse, K. Ohkubo, M. Kanai, *Chem. Sci.* **2019**, *10*, 3459–3465; h) Y. Hirao, Y. Katayama, H. Mitsunuma, M. Kanai, *Org. Lett.* **2020**, *22*, 8584–8588; i) S. Tanabe, H. Mitsunuma, M. Kanai, *J. Am. Chem. Soc.* **2020**, *142*, 12374–12381.
- [23] a) A. Gualandi, F. Calogero, M. Mazzarini, S. Guazzi, A. Fermi, G. Bergamini, P. G. Cozzi, *ACS Catal.* **2020**, *10*, 3857–3863; b) F. Calogero, A. Gualandi, S. Potenti, M. Di Matteo, A. Fermi, G. Bergamini, P. G. Cozzi, *J. Org. Chem.* **2021**, *86*, 7002–7009; c) A. Gualandi, G. Rodeghiero, R. Perciaccante, T. P. Jansen, C. Moreno-Cabrerizo, C. Foucher, M. Marchini, P. Ceroni, P. G. Cozzi, *Adv. Synth. Catal.* **2021**, *363*, 1105–1111; d) F. Calogero, S. Potenti, E. Bassan, A. Fermi, A. Gualandi, J. Monaldi, B. Dereli, B. Maity, L. Cavallo, P. Ceroni, P. G. Cozzi, *Angew. Chem. Int. Ed.* **2022**, *61*, e202114981. *Angew. Chem.* **2022**, *134*, e202114981.
- [24] Y.-L. Li, S.-Q. Zhang, J. Chen, J.-B. Xia, *J. Am. Chem. Soc.* **2021**, *143*, 7306–7313.
- [25] Y.-L. Li, W.-D. Li, Z.-Y. Gu, J. Chen, J.-B. Xia, *ACS Catal.* **2020**, *10*, 1528–1534.
- [26] H. Xie, B. Breit, *ACS Catal.* **2022**, *12*, 5, 3249–3255.
- [27] E. Speckmeier, T. Fischer, K. Zeitler, *J. Am. Chem. Soc.* **2018**, *140*, 45, 15353–15365.
- [28] a) M. A. Brydena, E. Zysman-Colman, *Chem. Soc. Rev.* **2021**, *50*, 7587–7680; b) A. Gualandi, M. Anselmi, F. Calogero, S. Potenti, E. Bassan, P. Ceroni, P. G. Cozzi, *Org. Biomol. Chem.* **2021**, *19*, 3527–3550.
- [29] The activation barrier for benzaldehyde was calculated being higher than that for acetaldehyde, but the regioselectivities of the reactions with these aldehydes are very similar; see: P. Liu, P. McCarren, P. H.-Y. Cheong, T. F. Jamison, K. N. Houk, *J. Am. Chem. Soc.* **2010**, *132*, 2050–2057.
- [30] P. R. McCarren, P. Liu, P. H.-Y. Cheong, T. F. Jamison, K. N. Houk, *J. Am. Chem. Soc.* **2009**, *131*, 6654–6655.
- [31] a) M. R. Chaulagain, G. J. Sormunen, J. Montgomery, *J. Am. Chem. Soc.* **2007**, *129*, 9568–9569; b) E. A. Colby, K. C. O'Brien, T. F. Jamison, *J. Am. Chem. Soc.* **2005**, *127*, 4297–4307.
- [32] H. Uoyama, K. Goushi, K. Shizu, H. Nomura, C. Adachi, *Nature* **2012**, *492*, 234–238.
- [33] M. Y. Wong, E. Zysman-Colman, *Adv. Mater.* **2017**, *29*, 1605444.
- [34] M. Streiter, T. G. Fischer, C. Wiebeler, S. Reichert, J. Langenickel, K. Zeitler, C. Deibel, *J. Phys. Chem. C* **2020**, *124*, 15007–15014.
- [35] P.-Z. Wang, J.-R. Chen, W.-J. Xiao, *Org. Biomol. Chem.* **2019**, *17*, 6936–6951.
- [36] DME is not suitable for Stern Volmer experiments and quenching analysis since the $[\text{NiCl}_2(n\text{Bu}_3\text{P})_2]$ complex is not stable under air when dissolved in this solvent.
- [37] H. Roth, N. Romero, D. Nicewicz, *Synlett* **2015**, *27*, 714–723.
- [38] The reduction potential of $[\text{NiCl}_2(n\text{Bu}_3\text{P})_2]$ was not reported in literature, to the best of our knowledge. However, the reduction potential of $[\text{NiCl}_2(\text{Pr}_3\text{P})_2]$ (–1.05; –1.25 V vs SCE) was reported in literature: G. Bontempelli, B. Corain, L. De Nardo, *J. Chem. Soc. Dalton Trans.* **1977**, 1887–1891.
- [39] M.-Y. Lee, C. Kahl, N. Kaeffer, W. Leitner, *JACS Au* **2022**, *2*, 573–578.
- [40] M. T. Haynes II, P. Liu, R. D. Baxter, A. J. Net, K. N. Houk, J. Montgomery, *J. Am. Chem. Soc.* **2014**, *136*, 17495–17504.